Check for updates

The saga of dyssynchrony imaging: Are we getting to the point

Elena Galli, Vincent Galand, Virginie Le Rolle, Marion Taconne, Adrien Al Wazzan, Alfredo Hernandez, Christophe Leclercq and Erwan Donal*

Department of Cardiology and Vascular Disease, Univ Rennes, CHU Rennes, Inserm, LTSI – UMR 1099, Rennes, France

Cardiac resynchronisation therapy (CRT) has an established role in the management of patients with heart failure, reduced left ventricular ejection fraction (LVEF < 35%) and widened QRS (>130 msec). Despite the complex pathophysiology of left ventricular (LV) dyssynchrony and the increasing evidence supporting the identification of specific electromechanical substrates that are associated with a higher probability of CRT response, the assessment of LVEF is the only imaging-derived parameter used for the selection of CRT candidates.

This review aims to (1) provide an overview of the evolution of cardiac imaging for the assessment of LV dyssynchrony and its role in the selection of patients undergoing CRT; (2) highlight the main pitfalls and advantages of the application of cardiac imaging for the assessment of LV dyssynchrony; (3) provide some perspectives for clinical application and future research in this field.

Conclusion: the road for a more individualized approach to resynchronization therapy delivery is open and imaging might provide important input beyond the assessment of LVEF.

1. Introduction

Cardiac resynchronisation therapy (CRT) has an established role in the management of patients with heart failure (HF), a severely reduced left ventricular ejection fraction (LVEF <35%) and a QRS > 130 msec, who remain symptomatic despite an optimized medical therapy [1].

However, 30%–40% of patients receiving CRT according to recommendations [1] do not experience significant LV reverse remodelling and improvement in LVEF [2].

In the last 20 years, significant efforts have been made for identifying imaging-derived parameters able to disclose the electromechanical substrates associated with CRT response, substantially increasing the knowledge of the pathophysiological mechanisms of LV dyssynchrony and potentially contributing to the improvement in the selection of CRT candidates.

This paper aims to 1) provide an overview of the evolution of cardiac imaging for the assessment of LV dyssynchrony and its role in the selection of patients undergoing CRT; 2) highlight the main pitfalls and advantages of the application of cardiac imaging for the

assessment of LV dyssynchrony; 3) provide some perspectives for clinical application and future research in this field.

2. Pathophysiology of left ventricular dyssynchrony

The loss of a nearly simultaneous LV contraction in patients with typical left bundle branch block and left ventricular dyssynchrony is associated with the presence of early septal activation, starting at low LV pressure, which does not contribute to LV ejection and stretches the lateral wall. The stretch of the lateral wall further delays shortening and causes a vigorous activation against a locally increased preload (3). This alternation of activation and stretch of opposite LV walls seen in the dyssynchronous heart promotes local modifications of the LV function at the molecular and cellular level (4), with redistribution of myocardial blood flow and oxygen uptake (5), and the development of differences in septal-to-lateral wall thickness (6, 7). This deleterious pathophysiological process can be reversed in the case of successful CRT and is associated with positive LV reverse remodelling. However, in some patients, LV dyssynchrony is not attributable to specific electromechanical substrates responsive to CRT, but to other causes such as ischemia or left ventricular hypocontractility, which are associated with poor or absent CRT response (8–10). In the following paragraphs we will try to underscore the progress of myocardial imaging in disclosing the specific mechanisms associated with LV dyssynchrony in order to improve patients' selection and CRT success.

3. Imaging for the selection of CRT candidates

The mechanism of action of CRT in patients with HF and widened QRS are far to be fully elucidated. This incomplete understanding of the pathophysiology of the disease can explain the variety of potential responses to CRT going from a spectacular LV reverse remodelling, often referred to as "CRT super-response" (11) to milder effects, and even worsening of LV function (12–14). This is probably because CRT is primarily designed to correct the conduction disorders corresponding to a widened QRS, but with the main aim to improve LV mechanical efficiency. In this context, the assessment of LV mechanical dyssynchrony through cardiac imaging has been proposed as an additive criterion to select CRT recipients.

3.1. Assessment of left ventricular opposite wall delay

The initial imaging studies on LV mechanical dyssynchrony were focused on the measure of opposite wall delay by different echocardiographic modalities.
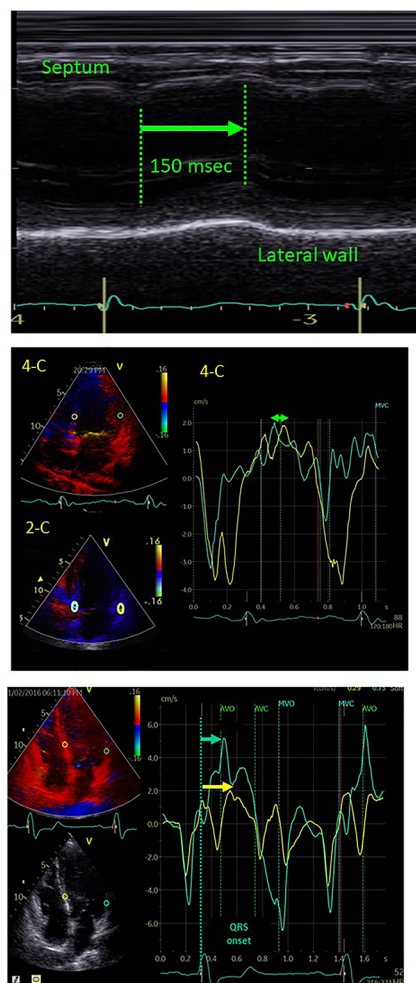
In 24 patients with heart failure, Pitzalis et al. showed that a septal-to-posterior motion delay ≥130 msec was able to predict LV reverse remodelling, with a positive predictive value of 80% and an accuracy of 85% (15). However, this approach was not suitable for patients with previous anterior or septal infarction and was plagued by poor temporal resolution (16). Successive studies, therefore, focused on tissue Doppler imaging and speckle tracking echocardiography for the assessment of LV dyssynchrony, by the estimation of opposite wall delay (17), or by focusing on the difference in peak systolic velocities of different myocardial regions (18–20) (**Figure 1**). Despite all these studies being able to show the good performance of echo-derived parameters for the prediction of CRT response in small, retrospective cohorts, the multicentric PROSPECT trial did not confirm the applicability of echocardiographic measures of dyssynchrony for the selection of CRT candidates (2).

These disappointing results are attributable to the poor reproducibility of the echo-derived analysis of dyssynchrony parameters (21), but also to the fact that the assessment of opposite wall delay is not able to disclose the complex pathophysiology related to CRT response. Computer simulation studies and clinical data have shown that there are several potential mechanisms associated with LV dyssynchrony, including electrical activation delay, regional differences in contractility and myocardial scar (9), so that only specific electromechanical substrates associated with a widened QRS are amenable to be corrected by CRT (**Table 1**).

3.2. Assessment of strain curves dynamics

The careful analysis of the dynamics and morphology of strain curves more than the evaluation of timings can provide further insight into the mechanisms of LV dyssynchrony and ease the identification of specific deformation patterns associated with CRT response. In 189 CRT candidates, the Multicentre study using strain delay index for predicting response to cardiac resynchronization therapy (MUSIC) study showed that in the case of preserved contractility and significant dyssynchrony, LV segments present a higher difference between the peak and end-systolic strain, which is a measure of segmental wasted energy. The global LV wasted energy is referred to as strain delay index (SDI) and has been shown to predict CRT response with an AUC of 0.88, a sensitivity of 92% and a specificity of 65% (22). A similar approach for the assessment of strain dynamics relies upon the semi-automatic analysis of strain integrals. Bernard et al. reported a significant heterogeneity of strain integrals in CRT-responders compared to non-responders. Moreover, these authors showed that the difference of strain integrals measured at strain peak and aortic valve closure, which represent the wasted energy of the LV myocardium, is higher in CRT-responders and is corrected by successful CRT (23) (**Figure 2**).

Starting from the visual analysis of strain curves obtained in a 4-chamber view in the septal and lateral wall, Risum et al. have shown that the "typical left bundle branch block" (LBBB) strain pattern is characterized by an early shortening of the septal wall,

Septal-to-posterior wall motion delay calculated as the shortest interval between the maximal posterior displacement of the septum and the maximal displacement of the left posterior wall using M-mode echocardiography in short-axis view at the papillary muscle level (Ref. 15).

Tissue Doppler signals are obtained from the apical 2- and 4-chamber view. The maximal time-to peak delay between the septum and the later wall or the anterior and posterior wall is assessed. We report here the delay between the septal and lateral wall in 4C-view.
(Ref. 18, 19).

Tissue Doppler Imaging signals are obtained form 4 left ventricular segments in apical 2-, 3- and 4-chamber views. The standard deviation of the time-to-peak myocardial systolic contraction is measured from the 12 left ventricular segments using the QRS onset as time reference point.
We report here the assessment of the time-to-peak contraction for the basal infero-septal (green arrow) and basal antero-septal segment (yellow arrow) (Ref 20)

FIGURE 1
Examples of the estimation of opposite wall delay in CRT candidates according to the main methods described in the literature. Upper panel: Pitzalis' method; Middle panel: Bax's method; Lower panel: Yu's method.

before the opening of the aortic valve, with concomitant stretch in the lateral wall. This early septal activation is followed by immediate lengthening (rebound stretch) and causes a delayed lateral wall peak contraction (Figure 3). This specific activation pattern has been shown to improve the prediction of LV reverse remodelling and prognosis after CRT (24). Computer simulation studies have demonstrated that the progressive decline in LV contractility is associated with a loss of the septal-to-lateral wall interplay typical of LBBB, such explaining the poor CRT-response in these patients (45). The sum of the posterolateral systolic prestretch and septal systolic rebound stretch, referred to as systolic stretch index (SSI) can be used to quantify the electromechanical substrate of dyssynchronous heart and has been shown to be associated with both CRT-response and prognosis (9, 25). Interestingly, an SSI > 2.6% was able to predict death or HF hospitalisation (HR: 2.08; 95% CI: 1.27 to 3.41, $p = 0.004$) and overall survival (HR 5.08; 95% CI: 1.94 to 13.31, $p < 0.001$) also in patients with a QRS width 120 to 149 ms or non-LBBB morphology (Figure 3).

The localisation of myocardial scar can also impact septal motion patterns in LBBB. In an experimental study, Aalen et al. have shown that the presence of lateral wall scar leads to the loss of septal rebound stretch, whereas extensive anterior ischemia increases rebound stretch (10), suggesting that scar localisation together with septal motion should be taken into account in the evaluation of LV dyssynchrony (Table 1).

3.3. The visual assessment of dyssynchrony: septal flash and apical rocking

Another approach to assess the unique contraction pattern typical of LBBB relies on the analysis of the contraction of opposite wall looking for the presence of septal flash (SF) (26) and/or apical rocking (ApR) (46).

The SF corresponds to the early septal thickening/thinning during the isovolumic systole and can be easily detected by M-mode parasternal long-axis view of by tissue Doppler imaging

TABLE 1 Summary of the main cited studies providing an overview of the role of imaging-derived parameters modalities in the field of CRT.

Assessment of LV opposite wall delay				
Authors/Journal – year/Ref	Population	Endpoints	Imaging parameters	Results
Pitzalis MV et al. J Am Coll Cardiol 2002. (15)	24 pts LVEF 24 ± 5%, QRS width 169 ± 16 msec, 20% ischemic	LVESV reduction > 15% at 6 months FU	Septal-to-lateral wall delay > 130 msec	AUC 0.95, PPV 80%, Sp 63%, Accuracy 85% for the prediction of LV reverse remodelling
Marcus GM et al. J Am Coll Cardiol 2005. (16)	79 pts LVEF 22 ± 7%, QRS width 159 ± 27 msec, 72% ischemic	LVESV reduction > 15% at 6 months FU	Septal-to-lateral wall delay > 130 msec	Se 24%, Sp 66%, PPV 29%, NPV 61% for the prediction of LV reverse remodelling
Søgaard P et al. J Am Coll Cardiol 2002. (17)	25 pts LVEF 29 ± 7%, QRS width 189 ± 23 msec, 44% ischemic	LVEF and GSCA improvement	Basal segment delayed contraction at TDI	Prediction of LVEF improvement: $r = 3.1$, $p < 0.01$; Prediction of GSCA improvement: $r = 3.3$, $p < 0.01$
Gorcsan J et al. Am J Cardiol 2004. (18)	29 patients LVEF 26 ± 6% %, QRS width 175 ± 34 msec, 44% ischemic	Acute LV stroke volume increase >15%	Antero-septum to posterior wall delay > 65 msec at TDI	Se 87%, Sp 100% for the prediction of acute of LV reverse remodelling
Bax JJ et al. J Am Coll Cardiol 2004. (19)	86 pts LVEF <40% QRS > 140 msec, 55% ischemic	1) LVESV reduction > 15% at 6 months FU 2) Clinical improvement	LV opposite wall delay > 65 msec at TDI	Se 92% and Sp 92% for the prediction of LV reverse remodelling; Se 80%, Sp 80% for the prediction of clinical improvement
Yu CM Am J Cardiol 2003. (20)	30 pts LVEF 23 ± 7%, QRS width 150 ± 18 msec, 40% ischemic	LVESV reduction > 15% at 6 months FU	Standard deviation of the time-to-peak systolic strain of 12 LV segments	Predictor of LV reverse remodelling ($\beta = -1.54$, p 0.007). Se and Sp 100% for the prediction of CRT response.
Assessment of LV strain dynamics and mechanical dyssynchrony				
Lumens J et al. Circ Cardiovasc Imaging 2015. (9)	191 pts LVEF 24 ± 6%, QRS width 159 ± 27 msec, 60% ischemic	Primary: HF hospitalization or overall death Secondary: overall deart, heart transplant or LV-assisted device	Systolic stretch index (SSI)	SSI ≥ 9.7% is an independent predictor of the primary endpoint (HR = 0.32; 95% CI: 0.19–0.53; $p < 0.001$) and secondary endpoint (HR = 0.28; 95% CI: 0.15–0.55, $p < 0.001$)
Lim P et al. Eur J Heart Fail 2011. (22)	189 pts LVEF 26 ± 8%, QRS width 151 ± 34 msec, 33% ischemic	LVESV reduction > 15% at 6 months FU	Strain delay index	AUC 0.80, Se 92%, Sp 65%, PPV 80%, NPV 84% for the prediction of LV reverse remodelling
Bernard A et al. J Am Soc Echocardiogr 2015. (23)	130 patients LVEF 27 ± 6%, QRS width 162 ± 23 msec, 38% ischemic	LVESV reduction > 15% at 6 months FU	Difference of strain integrals between AVC and strain peak (Diff$_{Int}$)	Higher Diff$_{int}$ in the lateral wall in responders
Risum N et al. J Am Coll Cardiol 2015. (24)	208 pts LVEF <35%, QRS width > 120 msec, 58% Ischemic	Cumulative death, left ventricular assist device, or heart transplantation	Typical vs. atypical LBBB strain patters	Absence of "Typical" LBBB strain pattern is an independent prognostic predictor: HR = 3.1; 95% CI: 1.64 to 5.88, $p < 0.005$
Gorcsan J et al. JACC Cardiovasc Imaging 2018. (25)	442 pts LVEF 25 ± 7%, QRS width 155 ± 21 msec, 47% Ischemic	Primary: HF hospitalization or death; Secondary: death	Systolic stretch index	SSI < 3.1% is an independent predictor of the primary endpoint (HR = 2.17; 95% CI: 1.45 to 3.24, $p < 0.001$) and secondary endpoint (HR = 4.06; 95% CI: 1.95 to 8.45, $p < 0.001$)
Parsai C et al. Eur Heart J 2009. (26)	161 pts LVEF 24 ± 7%, QRS width 156 ± 21 msec, 51% Ischemic	LVESV reduction > 10% at 6 months FU	Septal flash (SF)	Reversal of septal flash after CRT is associated with 100% reverse remodelling
Stankovic I et al. Eur Heart J Cardiovasc Imaging. 2017 (27)	1,060 patients LVEF 27 ± 7%, QRS width 170 ± 29 msec, 43% Ischemic	1) LVESV reduction > 15% at 6 months FU 2) Overall death	Septal flash/Apical rocking (ApR)	Reverse remodelling prediction: SF: Se = 70%, Sp = 74%, Accuracy = 77% ApR: Se = 84%, Sp = 79%, Accuracy = 82% Mortality prediction: SF: HR = 0.45, 95% CI: 0.34– 0.61, $p < 0.0001$ ApRock: HR = 0.40, 95% CI: 0.30–0.53, $p < 0.0001$)
Marsan NA et al. European Heart Journal 2009. (28)	35 patients LVEF 24 ± 8%, QRS width 145 ± 33 msec, 57% Ischemic	LVESV reduction > 15% at 6 months FU	16-segment time-to-maximum radial wall thickness assessed at CMR (16-SD); scar extent	Independent predictors of LV reverse remodelling 16-SD: OR = 6.3, 95% CI 3.1–9.9, $p < 0.001$ Scar: OR = 0.52, 95% CI 0.43–0.87, $p < 0.001$

(continued)

TABLE 1 Continued

Assessment of LV opposite wall delay				
Authors/*Journal – year*/Ref	Population	Endpoints	Imaging parameters	Results
Assessment of myocardial contractility and global left ventricular function				
Parsai C et al. *Eur Heart J 2009.* (29)	52 pts LVEF 24 ± 7%, QRS width 145 ± 24 msec, 44% Ischemic	LVESV reduction > 10% at 7 ± 1 months FU	DSE-induced SF	Prediction of LV reverse remodelling (R = 0.6, $p < 0.0001$)
Ciampi Q et al. *European Journal of Heart Failure 2009.* (30)	69 pts LVEF 27 ± 6%, QRS width 150 ± 27 msec, 55% Ischemic	LVESV reduction > 15% at 6 months FU	Contractile reserve at DSE	Best predictor of LV reverse remodelling: OR = 6.2, 95% CI: 1.4–27.6, $p < 0.015$
Delgado-Montero A et al. *Circ Cardiovasc Imaging 2016.* (31)	205 pts LVEF 24 ± 6%, QRS width 157 ± 26 msec, 63% Ischemic	Primary: death, circulatory support, or transplant Secondary: HF hospitalization or death	GLS, GCS	Independent predictors of the primary endpoint: GLS > −9%: HR = 2.91; 95% CI: 1.88–4.49, $p < 0.001$ GCS > −9%: HR = 3.73; 95% CI: 2.39–5.82, $p < 0.001$ Independent predictors of the secondary endpoint: GLS > −9%: HR = 2.10; 95% CI: 1.45–3.05, $p < 0.001$ GCS > −9%: HR = 3.25; 95% CI: 2.23–4.75, $p < 0.001$.
Khidir MJH et al. *Heart Rhythm 2018.* (32)	829 pts LVEF 27 ± 8%, QRS width 149 ± 30 msec, 60% Ischemic	Primary: overall death, heart transplantation, and LV assist device implantation Secondary: ventricular arrhythmias or appropriate ICD therapy	GLS	Independent predictor of the primary endpoint (HR = 1.075, 95% CI: 1.020–1.133, $p = 0.007$) but not of the secondary endpoint
van der Bijl P et al. *Eur Heart J Cardiovasc Imaging 2019.* (33)	1,185 pts LVEF 27 ± 8%, QRS width 155 ± 35 msec, 56% Ischemic	Overall death	≥15%↓LVESV and/or ≥5%↑|GLS| at 6-month FU	Independent predictors of overall death: ≥15%↓LVESV and ≥5% ↑|GLS|: HR = 0.47; 95% CI: 0.31–0.71, $p < 0.001$; ≥15%↓LVESV and <5%↑|GLS| or <15%↓LVESV and ≥5%↑|GLS|: HR = 0.57, 95% CI: 0.47–0.71, $p < 0.001$
Assessment of scar extension and localisation				
Delgado V et al. *Circulation 2011.* (34)	397 pts LVEF 25 ± 7%, QRS width 155 ± 33 msec, 100% Ischemic	HF hospitalization and overall death	LV radial dyssynchrony, discordant lead position, scar in the targeted segment	LV dyssynchrony: HR = 0.994, 95% CI: 0.992–0.998, $p = 0.001$ Discordant lead: HR = 2.086, 95%: 1.336–3.258, $p = 0.001$ Scar in the targeted segment: HR = 2.913, 95% CI: 1.740–4.877, $p < 0.001$
Khan FZ et al. *J Am Coll Cardiol 2012.* (35)	220 pts LVEF < 30%, QRS width > 130 msec, 56% ischemic	Primary: LVESV reduction >15% at 6 months FU. Secondary: overall death and HF hospitalization	LV lead position at the latest activated viable segment (Target group vs. non-target group)	Significant ΔLVESV in the target group vs. non-target group: −46 ± 33 vs. −26 ± 23 ml and better prognosis (log-rank $p = 0.031$)
Bose A et al. *J Cardiovasc Electrophysiol 2014.* (36)	160 patients LVEF 25 ± 7%, QRS width 159 ± 28 msec, 100% ischemic	Primary: HF hospitalization and overall death	Myocardial substrate at the site of LV lead by SPECT-MPI	Independent predictors of prognosis: scar at the LV lead: HR = 2.07, 95%CI: 1.14–3.74, $p = 0.015$ ischemia and scar at the LV lead: HR = 2.03 95% CI: 1.03–4.0, $p = 0.040$
Adelstein EC et al. *European Heart Journal 2011.* (37)	624 patients LVEF 24 ± 6%, QRS width 169 ± 33 msec	Primary: overall death; cardiac transplant, or mechanical circulatory support	Scar assessed at SPECT	Independent predictor of prognosis: Scar: HR = 1.8, 95% CI: 1.3–2.5, $p < 0.001$, unsuccessful LV lead implant: HR = 2.4, 95% CI: 1.4–4.2, $p < 0.001$)
Aalen JM et al. Eur Heart J 2020. (8)	220 pts LVEF <35%, QRS width 167 ± 21 msec, 35% ischemic	Primary: LVESV reduction >15% at 6 months FU. Secondary: overall death and heart transplantation	Septal-to-lateral wall work difference; scar localisation at MRI	Septal-to-lateral wall work difference (B = −0.011, $p < 0.0001$) and septal scar ($\beta = 0.42$, $p = 0.029$) are the main determinants of LV reverse remodelling and prognosis (AUC 0.88, Se 86%, Sp 84%, Accuracy 85%)
Importance of a comprehensive evaluation of cardiac function				
Moss AJ et al. *N Engl J Med 2009* (38)	1,820 patients LVEF < 30%, QRS width > 130 msec, 55% ischemic	Overall death, HF hospitalisation	LV size and function	
Carluccio E et al. *JACC Cardiovasc Imag 2011.* (39)	78 pts LVEF 26 ± 6%, QRS	1) Improvement in LVEF 2) Cardiac events	LV size	Indexed LVESVI > 103 ml/m^2 is an independent predictor of cardiac events (HR = 2.53, 95% CI: 1.17–5.44, $p = 0.017$)

(continued)

TABLE 1 Continued

Assessment of LV opposite wall delay				
Authors/*Journal – year/*Ref	Population	Endpoints	Imaging parameters	Results
	width 165 ± 30 msec, 33%ischemic			
Galli E et al. *Int J Cardiol 2021.* (40)	193 LVEF 28 ± 8%, QRS width 167 ± 21 msec, 33% ischemic	Overall death, heart transplantation, LV-assisted device implantation	Diastolic dysfunction degree	Grade I diastolic dysfunction portends a better prognosis (HR = 0.37, 95%CI: 0.14–0.96; log-rank p vs. grade II-III diastolic dysfunction <0.0001)
Kuperstein R et al. *Circ Heart Fail 2014.* (41)	1,785 pts LVEF < 35%, QRS width > 130 msec	HF hospitalisation or overall death	LA volume	LA volume > 52 ml/m^2 is an independent prognostic predictor: HR = 1.69, 95% CI: 1.35–2.11, p < 0.001, log-rank p < 0.001
Galli E et al. *Eur Heart J Cardiovasc Imaging 2022.* (42)	221 pts LVEF < 35%, QRS width > 165 ± 26 msec, ischemic 33%	LVESV reduction >15% at 6 months FU LVEDV reduction > 10% at 6 months FU	LA reservoir strain	Independent predictor of systolic (β-0.14, p = 0.049) and LV diastolic remodelling (β = −0.17, p = 0.001)
Damy T et al. *J Am Coll Cardiol 2013.* (43)	688 pts from CARE-HF, 345 receiving CRT Median LVEF 24 (21–28) %, QRS > 130 msec, 33% ischemic	Overall mortality	TAPSE	TAPSE <17 mm is an independent prognostic predictor (log-rank p < 0.0001) in both CRT and medical treated patients
Rapacciuolo A et al. *Clin Cardiol 2016.* (44)	227 pts LVEF28 ± 6%, QRS width > 162 ± 26 msec, ischemic 41%	LVESV reduction >15% at 6 months FU	TAPSE	TAPSE > 17 mm is an independent predictor of LV remodelling; Se 68%, Sp 54%; OR = 1.97, 95% CI: 1.03–3.80, p < 0.05

ApR, apical rocking; AUC, area under the curve; AVC, aortic valve closure; CI, confidence interval; CMR, cardiac magnetic resonance; CRT, cardiac resynchronization therapy; DSE, dobutamine stress echocardiography; Diff$_{int}$, difference of strain integrals between AVC and strain peak; FU, follow-up; GCS, global circonferential strain; GLS, global longitudinal strain; GSCA, global systolc contraction amplitude; HF, heart failure; HR, hazard ratio; ICD, intracardiac defibrillator; LA, left atrium; LBBB, left bundle branch block; LV, left ventricle; LVEF, left ventricular ejection fraction; LVEDV, left ventricular end-diastolic volume; LVESV, left ventricular end-systolic volume; MPI, myocardial perfusion imaging; 6 MWT, six-minute = walking test; NYHA, New York Heart Association functional class; NPV, negative predictive value; OR, odds ratio; PPV, positive predictive value; Se, sensitivity; SF, septal flash; SPECT, single-photon emission computed tomography; Sp, specificity; SSI, systolic stretch index; SV stroke volume; TAPSE, tricuspidannular plane systolic excursion; TDI, tissue Doppler imaging.

in short or long parasternal long axis view (26, 47). The ApR corresponds to apical transverse motion due to the early septal contraction followed by the delayed activation of the lateral wall (46). Both these parameters have shown to portend LV residual contractility in CRT-candidates (48), to predict CRT-response and long-term survival after CRT implantation, and to improve the prognostic stratification of guideline-based patients' selection (27).

Moreover, these motion patterns have proven to predict CRT-response in patients with chronic right ventricular pacing needing a pacemaker upgrade to CRT (49).

However, the correct identification of septal flash and apical rocking in CRT candidates is strictly limited by the experience of the echo-reader. In a small monocentric study, Mada et al. have shown that the semi-automatic detection of these specific contraction patterns by speckle tracking echocardiography performed better than novice echo-readers for the identification of SF/ApR (50) (**Table 1**).

Despite the visual assessment of LV dyssynchrony is often performed by echocardiography, other imaging modalities such as cardiac magnetic resonance (CMR) and single photon emission computed tomography (SPECT) might be used to detect LV mechanical discoordination. Both these imaging modalities allow the contemporary assessment of scar localization and viability, and they might provide an interesting approach for t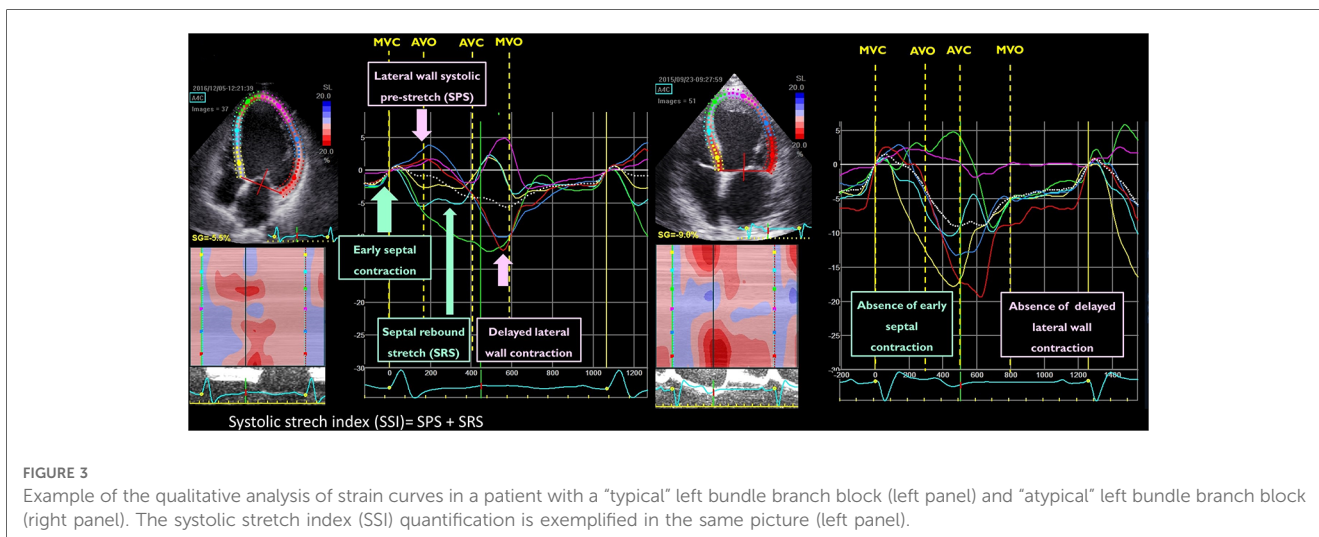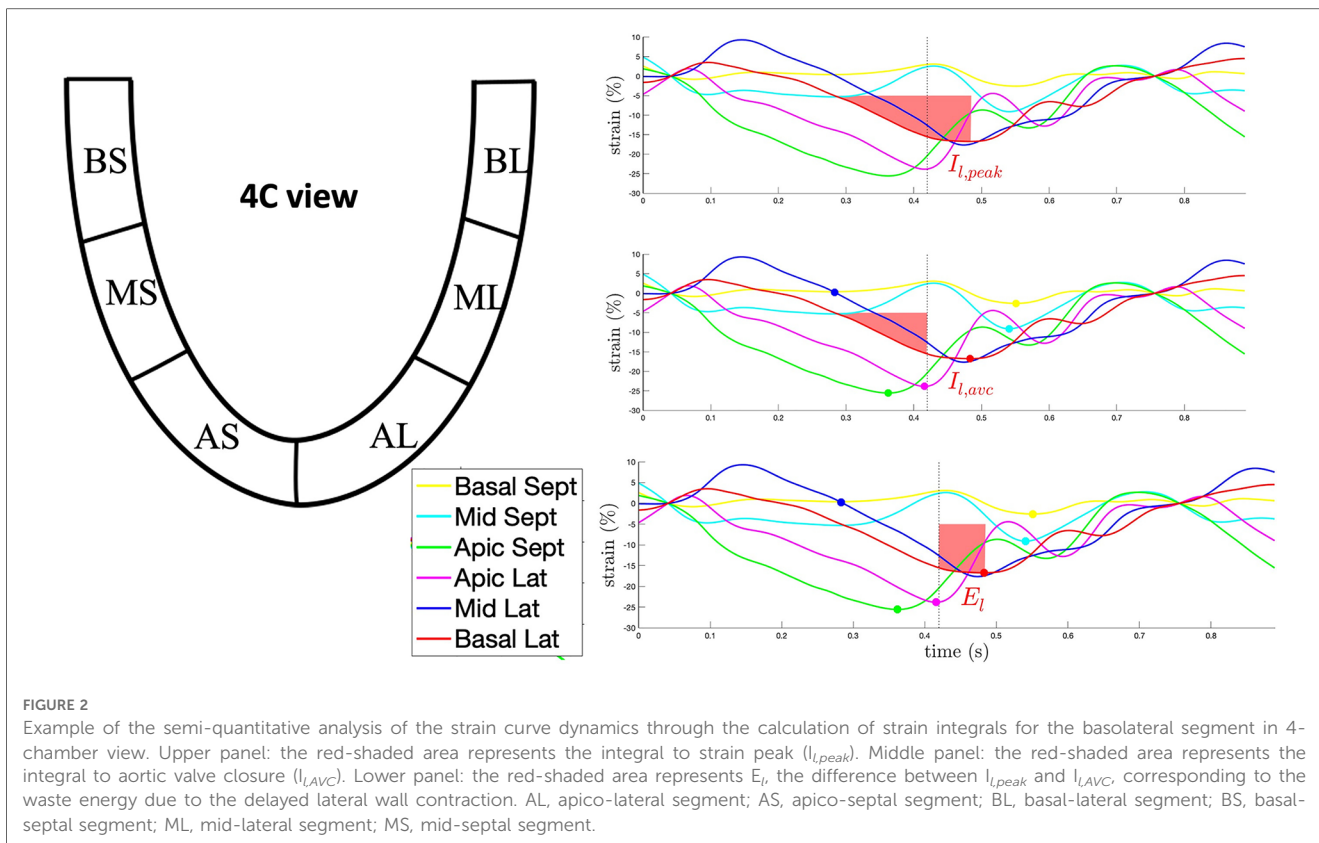he evaluation of CRT candidates before device implantation (28, 51, 52). However, these imaging modalities are plagued by a poor temporal resolution which can impact the refined assessment of LV dyssynchrony, thus favoring echocardiography for this specific purpose (53).

3.4. Assessment of myocardial contractility and global left ventricular function

Myocardial contractility and scar localisation are two important parameters associated with CRT-response.

Dobutamine stress echocardiography (DSE) can be used to identify the presence of contractile reserve and LV dyssynchrony in CRT-candidates (29, 30). In 69 CRT candidates undergoing DSE, Ciampi et al. showed that the presence of contractile reserve defined by a wall motion score index variation >0.20 is associated with significant LV reverse remodelling and survival after CRT delivery (30). Low-dose DSE is also able to disclose/ accentuate the presence of visual LV dyssynchrony, making the detection of dyssynchrony much easier at peak stress, and helping the identification of CRT responders (29).

The measure of global LV function parameters at baseline might provide useful information for the prediction of CRT response. Several single-centre studies (31–33, 54) and two recent large metanalyses (55, 56) showed that LV global longitudinal strain measured before CRT delivery is both a predictor of CRT-

FIGURE 2
Example of the semi-quantitative analysis of the strain curve dynamics through the calculation of strain integrals for the basolateral segment in 4-chamber view. Upper panel: the red-shaded area represents the integral to strain peak ($I_{l,peak}$). Middle panel: the red-shaded area represents the integral to aortic valve closure ($I_{l,AVC}$). Lower panel: the red-shaded area represents E_l, the difference between $I_{l,peak}$ and $I_{l,AVC}$, corresponding to the waste energy due to the delayed lateral wall contraction. AL, apico-lateral segment; AS, apico-septal segment; BL, basal-lateral segment; BS, basal-septal segment; ML, mid-lateral segment; MS, mid-septal segment.

FIGURE 3
Example of the qualitative analysis of strain curves in a patient with a "typical" left bundle branch block (left panel) and "atypical" left bundle branch block (right panel). The systolic stretch index (SSI) quantification is exemplified in the same picture (left panel).

induced reverse remodelling and prognosis. In 205 HF patients referred for CRT implantation, Delgado-Monteiro et al. showed that a GLS>|−9%| was an independent predictor of a composite endpoint including death, circulatory support implantation and heart transplantation (HR: 2.91; 95% CI: 1.88–4.49; $p < 0.001$). Interestingly, the predictive value of this cut-off was maintained in patients with intermediate QRS width (120–150 msec), thus helping to refine the selection of patients with a class II indication for CRT implantation (31). The analysis of 1,185 patients from the Leiden CRT registry showed that some subjects can present a discordant CRT response, defined as an improvement in LVESV (left ventricular end-systolic volume) or CRT. The absence of increase in GLS despite the positive LV reverse remodelling might be attributed to an effective resynchronization of the LV ventricle, without concomitant increase in the contractile reserve. Patients with concomitant improvement in LVESV and CRT had the best prognosis [hazard ratio (HR) 0.47; 95% CI: 0.31–0.71, $p < 0.001$], whereas patients with a discordant improvement showed an intermediate survival benefit from CRT (33) (**Table 1**).

3.5. Assessment of scar extension and localisation

In patients with ischemic cardiomyopathy, the extension and localisation of myocardial scar significantly impact CRT response essentially in two ways: (1) the LV lead placement at areas of scar is associated with poor clinical and echocardiographic response to CRT (34, 35); (2) the higher is the scar burden, the lower is the residual LV contractility (10, 30).

As a matter of fact, in the Multicenter Automatic Defibrillator Implantation Trial with Cardiac Resynchronization Therapy (MADIT-CRT), ischemic cardiomyopathy emerged as an independent predictor of LV remodelling after CRT (57). Moreover, ischemic aetiology is associated with a worse prognosis and higher rate of HF hospitalisation in CRT candidates (58).

Cardiac imaging can have a pivotal role in the assessment of myocardial scar. In the landmark randomized TARGET trial, Khan et al.; showed that the positioning of the LV lead in a site far from LV scar and with significant residual contractility (defined as a >10% amplitude of the corresponding radial strain trace) was associated with a higher percentage of CRT response (70 vs. 55%, $p < 0.031$) and a significantly better survival (log rank $p = 0.002$). Nevertheless, when compared with scar assessment at cardiac magnetic resonance (CMR), the predictive value of segmental radial strain for the identification of myocardial scar is low (sensitivity 33% and specificity 72%) (59), suggesting the usefulness of a multimodality imaging approach to plan and ease CRT implantation.

Specifically, echocardiography can assess mechanical dyssynchrony, whereas CMR can quantify the extent and localization of myocardial scar.

Aalen et al. have shown that the localization of myocardial scar in the septum or in the lateral wall can impact LV dyssynchrony patterns at strain echocardiography (10).

If CMR is not available or contraindicated, SPECT might be applied for the localization of the scar and to assess viability (36, 51). In CRT candidates, the quantification of scar burden by SPECT has been associated with CRT response and prognosis (37). However, in the presence of normal coronary artery and LBBB, SPECT can display perfusion defects in the septal and apical segments. These perfusion abnormalities are due to the relative septal hypoperfusion, compared to the lateral wall and can be disclosed by the measure of the absolute regional myocardial perfusion at positron emission tomography (60).

Computed tomography (CT) can be used to analyse the individual's coronary venous anatomy and identify the best pacing site. Moreover, CT might be an alternative to CMR or SPECT to evaluate myocardial perfusion and scar, especially when these other imaging modalities are not available (61).

Despite the interesting perspectives provided by multi-modality (MMI) in CRT (62), 2 large randomized trials applying a combination of echocardiography, CMR and CT did not show any survival benefit of the multi-modality imaging-derived approach vs. the standard approach for CRT implantation (63, 64). Nevertheless, these studies showed that patients receiving the LV lead in the optimal site had better LV remodelling and survival after CRT, supporting the usefulness of a multimodality imaging approach at least in selected cases.

In addition, both these studies focused on the localisation of the myocardial scar in the lateral wall and neglected the value of septal scar and of the septal-to-lateral wall interplay that has shown to be a key element to understand the pathophysiology of LBBB and predict CRT response and prognosis (8, 10).

In 200 CRT recipients, the septal-to-lateral wall difference in myocardial work, emerged as an independent predictor of CRT response with area under the curve (AUC) of 0.77 (95% CI: 0.70–0.84). Nevertheless, the combination of work difference and septal viability increased the AUC to 0.88 (95% CI: 0.81–0.95). Interestingly, the predictive power of a combination of work assessment and septal scar was superior to QRS width for the prediction of LV remodelling after CRT and was an independent predictor of prognosis HR (0.21, 95% CI: 0.072–0.61) (8). These results underscore the importance of a combination of viability and septal-to-lateral wall dynamics for the evaluation of CRT candidates (**Figure 4** and **Table 1**).

4. The importance of a comprehensive evaluation of cardiac function

The imaging-driven analysis of CRT candidates is substantially focused on the assessment of LV function. Nevertheless, an increasing amount of literature shows the importance of a comprehensive approach when imaging CRT candidates for both the identification of CRT-responders and prognostic stratification.

The presence of an extensive LV remodelling before CRT delivery, with more severe LV dysfunction and significant LV dilatation is associated with poor prognosis and to less LV ejection fraction improvement (38, 39).

The assessment of diastolic function is particularly challenging in CRT candidates. Despite the application of the algorithm proposed by Nagueh et al. is discouraged in patients with LV conductions disturbances (65), Andersen OA et al. have shown that this approach is able to identify patients with elevated LV filling pressure against the invasive gold standard also in the case of LBBB or paced rhythm (66).

Previous studies have shown that CRT doesn't influence LV relaxation and successful CRT does not seems to impact the prevalence of diastolic dysfunction (DD) in CRT responders (40, 67). Nevertheless, the degree of DD in CRT candidates is an independent predictor of mortality (HR 6.04; 95% CI: 2.32–15.77 and HR 4.64, 95%CI: 1.49–14.39 for grade II and III DD, respectively) and unsuccessful CRT is associated with an increased prevalence of grade III DD (40).

The left atrium (LA) reflects the cumulative effect of LV filling pressure over time. In the MADIT-CRT trial, CRT was associated with a significant reduction of LA volume, which portended a substantial reduction in atrial tachyarrhythmias (68). In the same cohort, LA indexed volume >52 ml/m^2 and the lack of LA remodelling after CRT were both associated with a higher hazard
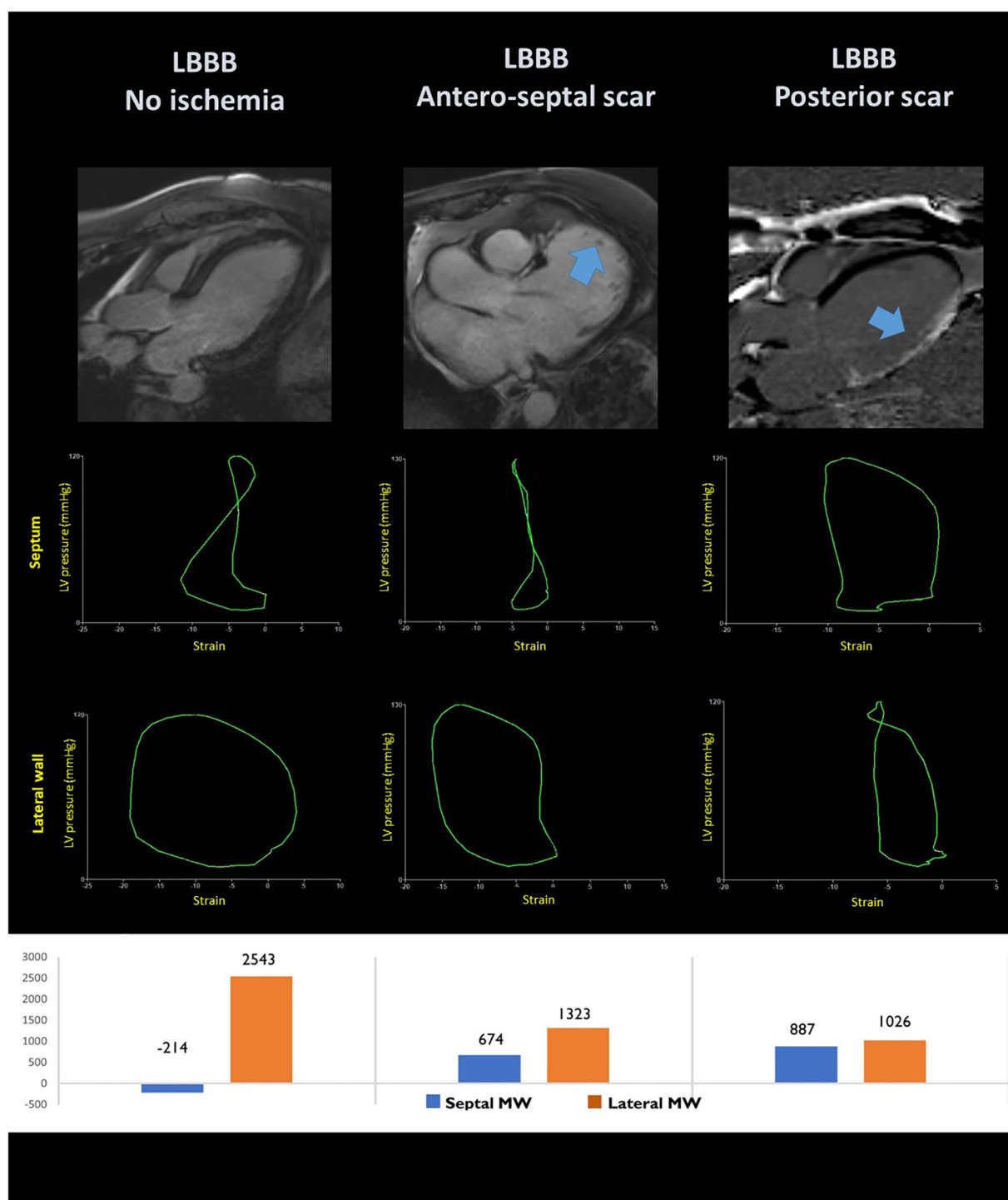
FIGURE 4
Pressure-loops analysis in the septal and lateral segments of patients with left bundle branch block without ischemic heart disease (left panel); with anteroseptal scar (central panel) and lateral wall scar (right panel). The corresponding localisation of the myocardial scar is shown at MRI late gadolinium enhancement in the upper panels.

of HF and mortality (41). Together with the assessment of LA size, the evaluation of LA reservoir strain (LARS) by speckle tracking echocardiography provides information on the effects of CRT on the LA. CRT is associated with a significant improvement in LARS in responders (42, 69) and baseline LARS is and independent predictor of both LV systolic and diastolic

remodelling at 6-month follow-up ($r = -0.14$, $p = 0.049$, $r = -0.17$, $p = 0.002$, respectively (42).

Because the main determinants of LARS are diastolic function and LV longitudinal function, LARS might allow a comprehensive assessment of both the systolic and diastolic LV impairment: the more impaired LARS, the more advanced is the ongoing left

FIGURE 5
A comprehensive approach to guide CRT implantation.
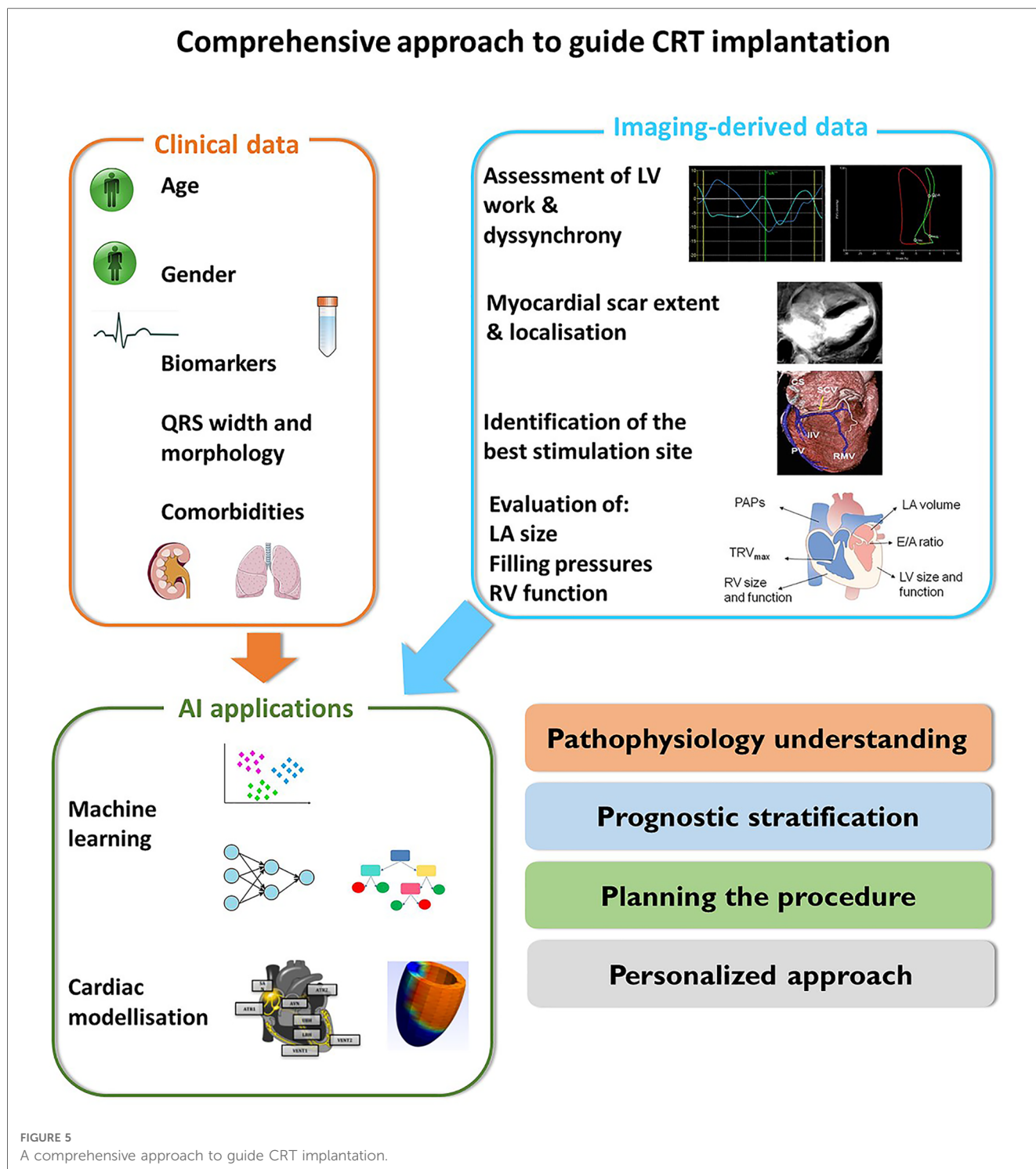
ventricular disease, and the less likely is CRT-induced reverse remodelling.

Finally, the relationship between RV function and left ventricular remodelling after CRT is object of debate. In a large meta-analysis of 16 studies, including 1,764 patients, Sharma et al. underscored that baseline RV function as assessed by tricuspid annular plane systolic excursion (TAPSE), RV fractional area change (FAC), RV strain or RV ejection fraction does not determine response to CRT as assessed by change in LVEF (70).

Nevertheless, more recent papers question these results by showing that RV dysfunction is predictor of poor prognosis in CRT candidates (43, 44). Interestingly, in an experimental model of LBBB Storsen et al. observed that LBBB causes an abnormal RV free wall motion pattern that is reversed after successful CRT only in the case of preserved RV function (71).

This might be attributable to the LV/RV interdependence through the LV septum, but can also be influenced by the effect of severe LV dysfunction on mitral regurgitation, filling pressure,

TABLE 2 Summary of the main cited studies providing an overview of the role of machine learning in the field of CRT.

Authors/ Journal – year/ Ref	Population	Endpoints	Methods	Parameters	Results
Donal E et al. *JACC Cardiovasc Imaging 2019.* (75)	154 pts LVEF < 35%, QRS width > 120 msec	LVESV reduction >15% at 6 months FU	Random Forest and Monte Carlo cross-validation	60 features from semi-automatic strain trace analysis, QRS width, visual Lv dyssynchrony	Extraction of 6 main features with an AUC 0.804 (0.77–0.94) for the prediction of LV reverse remodelling
Gallard A. et al. *Int J Cardiovasc Imaging 2021.* (76)	221 pts LVEF < 35%, QRS ≥120 msec	LVESV reduction >15% at 6 months FU	Random Forest	Features from echocardiography, strain traces analysis, QRS width, LV dyssynchrony	The combination of SF, E, E/A, E/e′, QRS width, LVESV and 8 features obtained from strain curves predicted LV reverse remodelling with an AUC of 0.81 ± 0.05
Gallard A et al. *PloS One 2021.* (77)	161 pts LVEF < 35%, QRS width > 120 msec	LVESV reduction >15% at 6 months FU	Random Forest	158 features from semi-automatic strain trace analysis, QRS width, LVEF	20 main features from strain analysis are the best predictors of LV reverse remodelling. 50% of these features are derived from the 4-chamber strain.
Cikes M et al. *Eur J Heart Fail 2019.* (78)	1,106 LVEF ≤ 30%, QRS width ≥130 ms	Overall death or HF hospitalisation	Multiple Kernel Learning and K-means clustering	Four phenogroups	Two phenogroups with better prognosis (HR = 0.35, 95% CI: 0.19–0.64, *p* < 0.0001 and HR = 0.36, 95% CI: 0.19–0.68, *p* = 0.001)
Galli E et al. *J Am Soc Echocardiogr 2021.* (79)	193 pts LVEF 29 ± 8%, QRS width 167 ± 21, 33% ischemic	Primary: heart transplantation, LV-assisted device implantation overall death	k-medoid, Boruta algorithm, random forest	28 clinical, biological and echo-derived variables; two phenogroups	Prognostic value of the main 8 variables: AUC 0.84 (0.75–0.93); Two phenogroups with different prognosis: HR = 4.70, 95% CI: 2.1–10.0, *p* < 0.0001; log-rank *p* < 0.0001)
Bivona DJ et al. *Heart Rhythm 2022.* (80)	200 pts LVEF 24.0 (17.7–30.5)%, QRS 58 (142–175) msec, 43.5% ischemic	1) Reduction of LVESV at 6 months FU 2) Survival	k-means method and Gaussian mixture model	39 features derived from CMR and biology	3 clusters able to predict CRT response and prognosis

AUC, area under the curve; CI, confidence interval; CMR, cardiac magnetic resonance; FU, follow-up; HF, heart failure; HR, hazard ratio; LV, left ventricle; LVEF, left ventriculare ejection fraction; LVESV, left ventricular end-systolic volume.

tricuspid regurgitation and pulmonary pressure (72) (**Figure 5** and **Table 1**).

5. Potential applications for artificial intelligence in CRT

Artificial intelligence (AI) is focused on the application of computational algorithms to huge amounts of data to identify patterns between variables that are not disclosed by the application of standard statistical methods (73). This approach seems particularly interesting in the field of CRT, where the high heterogeneity of CRT-candidates is probably the main determinant of the well-known wide variability in clinical benefit and outcomes (74).

In 154 CRT candidates, our group showed that the application of a random forest method (RF) and Monte Carlo cross validation allowed the identification of 6 strain-derived variables that were able to predict CRT-response with an AUC of 0.80 (95% CI: 0.77 to 0.94) (75).

By the analysis of a larger multicentric population of 323 CRT-candidates, Gallard et al. strengthened previous results and demonstrated that the application of a multifeatured learning method including visual LV dyssynchrony, standard echocardiographic parameters and strain-derived data was able to improve the prediction of CRT-response compared to the simple analysis of QRS duration, with an overall AUC or 0.81 (76).

Moreover, the semi-automatic analysis of strain traces and the subsequent application ML algorithms might be helpful to disclose relevant information that are not evident from the simple visual analysis on strain curves. The application of different methods such as out-of-bag random forest, wrapping and filtering to strain traces obtained in 4-, 3- and 2-chamber views has shown that the most important features are calculated from the 4-chamber view, essentially from the analysis of the antero-septal and basal-septal segment (77).

The application of an unsupervised ML algorithm to 1,106 HF patients from the MADIT-CRT trial was able to identify 4 phenogroups of patients, having different CRT-response and prognosis (78). Interestingly, the analysis of left atrial, LV and right ventricular morphology and function added significant information for the classification of patients. Using both supervised and unsupervised ML methods, Galli et al. were able to underscore the value of right ventricle-derived parameters for the prediction of CRT response and survival. This approach was able to reliable predict CRT response and outcome with an AUC or 0.81 (95% CI: 0.74–0.87) and 0.84 (95% CI: 0.75–0.93), respectively (79).

Similarly, the application of a clustering approach (k-means method and Gaussian mixture model) to clinical and CMR-derived features was also able to stratify CRT-candidates in three survival groups. Interestingly, the addition of CRT-volumetric response to selected pre-CRT data significantly increased the performance of the model for the prediction of prognosis (AUC 0.78 ± 0.04 vs. 0.86 ± 0.02) (80).

Although it is difficult to directly compare classifier performances because different datasets and ML models were used in these studies, these results show the added value of multivariate analysis for the prediction of CRT response.

Computer models represents another interesting application to merge imaging and ECG-derived data to drive computer simulation for the pathophysiological understanding of left ventricular dyssynchrony, improve response to CRT, and for the planning of CRT delivery. These models range from the simple bidimensional representation of LV function (81, 82), to complex 3D-models including the analysis of the molecular, electrical and mechanical properties of the myocardium (83, 84).

Moreover, the combination of clinical and model-derived data might contribute to enhance the pathophysiology understanding of CRT and also increase the accuracy in the prediction of LV remodelling and prognosis in CRT candidates (85).

The computational modelling of LV dyssynchrony relies on the merge of several different competences from imaging and electrophysiology to numerical analysis (**Figure 5**). The main challenge in this field is the large need of clinical validation, followed by the production of user-friendly tools that allow the analysis of data in a clinically useful time frame (86). The final goal is to merge clinical data and computer simulations to develop digital twins that are able to replicate the specific patient's heart disease and simulates the effect of CRT delivery (87) (**Table 2**).

The application of AI in medicine sounds appealing in several clinical scenarios including CRT because of its intrinsic capacity of analysing a huge amount of heterogeneous data and providing useful outcomes for diagnosis, management and prognosis. AI might therefore provide a fundamental contribution to the development of precision medicine and to a personalized approach to patients' care (88). However, several concerns exist about the wide application of AI in the health care system. These issues goes from the quality and transparency of data, to complex technical issues, to ethical and political concerns and need to be solved to provide a safe and fair application of AI in the field of medicine (73, 89).

Conclusions

Cardiac resynchronization therapy has a pivotal role for the management of patients with systolic heart failure and wide QRS. In the recent years, the excessive relevance given to the concept of "non-response" to CRT seems to contribute to the substantial underuse of the device, so that up-to two third of patients needing the CRT according to recommendations are not implanted (90).

This review provides an insight on the progresses of imaging in the field of CRT and underscore the need of a comprehensive approach which is useful to (1) disclose the electromechanical substrates more suitable to respond to CRT; (2) identify imaging pattern that are associated with good CRT response also in patients with unclassical indications; (3) emphasize the relevance of a global assessment of cardiac function including the evaluation of filling pressure, LA size and function, and RV function; (4) underscore the potentiality of AI to merge clinical, electrophysiological and imaging-derived data with the purpose of proposing patient's tailored strategies.

The final goal of this holistic approach to CRT is to individualize the treatment and to optimize CRT delivery.

Conflict of interest

The authors declare that the research was conducted in the absence of any commercial or financial relationships that could be construed as a potential conflict of interest.

Publisher's note

All claims expressed in this article are solely those of the authors and do not necessarily represent those of their affiliated organizations, or those of the publisher, the editors and the reviewers. Any product that may be evaluated in this article, or claim that may be made by its manufacturer, is not guaranteed or endorsed by the publisher.

References

1. Glikson M, Nielsen JC, Kronborg MB, Michowitz Y, Auricchio A, Barbash IM, et al. 2021 ESC guidelines on cardiac pacing and cardiac resynchronization therapy. *Eur Heart J.* (2021) 42(35):3427–520. doi: 10.1093/eurheartj/ehab364

2. Chung ES, Leon AR, Tavazzi L, Sun JP, Nihoyannopoulos P, Merlino J, et al. Results of the predictors of response to CRT (PROSPECT) trial. *Circulation.* (2008) 117(20):2608–16. doi: 10.1161/CIRCULATIONAHA.107.743120

3. Sweeney MO, Prinzen FW. Ventricular pump function and pacing: physiological and clinical integration. *Circ Arrhythm Electrophysiol.* (2008) 1(2):127–39. doi: 10.1161/CIRCEP.108.777904

4. Kirk JA, Kass DA. Cellular and molecular aspects of dyssynchrony and resynchronization. *Heart Fail Clin.* (2017) 13(1):29–41. doi: 10.1016/j.hfc.2016.07.003

5. Delhaas T, Arts T, Prinzen FW, Reneman RS. Regional fibre stress-fibre strain area as an estimate of regional blood flow and oxygen demand in the canine heart. *J Physiol.* (1994) 477 (Pt 3):481–96. doi: 10.1113/jphysiol.1994.sp020209

6. Cvijic M, Duchenne J, Ünlü S, Michalski B, Aarones M, Winter S, et al. Timing of myocardial shortening determines left ventricular regional myocardial work and regional remodelling in hearts with conduction delays. *Eur Heart J Cardiovasc Imaging.* (2018) 19(8):941–9. doi: 10.1093/ehjci/jex325

7. Prinzen FW, Cheriex EC, Delhaas T, van Oosterhout MF, Arts T, Wellens HJ, et al. Asymmetric thickness of the left ventricular wall resulting from asynchronous electric activation: a study in dogs with ventricular pacing and in patients with left bundle branch block. *Am Heart J.* (1995) 130(5):1045–53. doi: 10.1016/0002-8703 (95)90207-4

8. Aalen JM, Donal E, Larsen CK, Duchenne J, Lederlin M, Cvijic M, et al. Imaging predictors of response to cardiac resynchronization therapy: left ventricular work asymmetry by echocardiography and septal viability by cardiac magnetic resonance. *Eur Heart J.* (2020) 41(39):3813–23. doi: 10.1093/eurheartj/ehaa603

9. Lumens J, Tayal B, Walmsley J, Delgado-Montero A, Huntjens PR, Schwartzman D, et al. Differentiating electromechanical from non-electrical substrates of mechanical discoordination to identify responders to cardiac resynchronization therapy. *Circ Cardiovasc Imaging.* (2015) 8(9):e003744. doi: 10.1161/CIRCIMAGING.115.003744

10. Aalen JM, Remme EW, Larsen CK, Andersen OS, Krogh M, Duchenne J, et al. Mechanism of abnormal septal motion in left bundle branch block: role of left ventricular wall interactions and myocardial scar. *JACC Cardiovasc Imaging.* (2019) 12(12):2402–13. doi: 10.1016/j.jcmg.2018.11.030

11. Hsu JC, Solomon SD, Bourgoun M, McNitt S, Goldenberg I, Klein H, et al. Predictors of super-response to cardiac resynchronization therapy and associated improvement in clinical outcome: the MADIT-CRT (multicenter automatic defibrillator implantation trial with cardiac resynchronization therapy) study. *J Am Coll Cardiol.* (2012) 59(25):2366–73. doi: 10.1016/j.jacc.2012.01.065

12. Tayal B, Sogaard P, Delgado-Montero A, Goda A, Saba S, Risum N, et al. Interaction of left ventricular remodeling and regional dyssynchrony on long-term prognosis after cardiac resynchronization therapy. *J Am Soc Echocardiogr.* (2017) 30 (3):244–50. doi: 10.1016/j.echo.2016.11.010

13. Ruschitzka F, Abraham WT, Singh JP, Bax JJ, Borer JS, Brugada J, et al. Cardiac-resynchronization therapy in heart failure with a narrow QRS complex. *N Engl J Med.* (2013) 369(15):1395–405. doi: 10.1056/NEJMoa1306687

14. Ichibori H, Fukuzawa K, Kiuchi K, Matsumoto A, Konishi H, Imada H, et al. Predictors and clinical outcomes of transient responders to cardiac resynchronization therapy: transient responder to CRT. *Pacing Clin Electrophysiol.* (2017) 40(3):301–9. doi: 10.1111/pace.13023

15. Pitzalis MV, Iacoviello M, Romito R, Massari F, Rizzon B, Luzzi G, et al. Cardiac resynchronization therapy tailored by echocardiographic evaluation of ventricular asynchrony. *J Am Coll Cardiol.* (2002) 40(9):1615–22. doi: 10.1016/S0735-1097(02) 02337-9

16. Marcus GM, Rose E, Viloria EM, Schafer J, De Marco T, Saxon LA, et al. Septal to posterior wall motion delay fails to predict reverse remodeling or clinical improvement in patients undergoing cardiac resynchronization therapy. *J Am Coll Cardiol.* (2005) 46(12):2208–14. doi: 10.1016/j.jacc.2005.05.095

17. Søgaard P, Egeblad H, Kim WY, Jensen HK, Pedersen AK, Kristensen BØ, et al. Tissue Doppler imaging predicts improved systolic performance and reversed left ventricular remodeling during long-term cardiac resynchronization therapy. *J Am Coll Cardiol.* (2002) 40(4):723–30. doi: 10.1016/S0735-1097(02)02010-7

18. Gorcsan J, Kanzaki H, Bazaz R, Dohi K, Schwartzman D. Usefulness of echocardiographic tissue synchronization imaging to predict acute response to cardiac resynchronization therapy. *Am J Cardiol.* (2004) 93(9):1178–81. doi: 10. 1016/j.amjcard.2004.01.054

19. Bax JJ, Bleeker GB, Marwick TH, Molhoek SG, Boersma E, Steendijk P, et al. Left ventricular dyssynchrony predicts response and prognosis after cardiac resynchronization therapy. *J Am Coll Cardiol.* (2004) 44(9):1834–40. doi: 10.1016/j. jacc.2004.08.016

20. Yu CM, Fung WH, Lin H, Zhang Q, Sanderson JE, Lau CP. Predictors of left ventricular reverse remodeling after cardiac resynchronization therapy for heart failure secondary to idiopathic dilated or ischemic cardiomyopathy. *Am J Cardiol.* (2003) 91(6):684–8. doi: 10.1016/S0002-9149(02)03404-5

21. Hawkins NM, Petrie MC, Burgess MI, McMurray JJV. Selecting patients for cardiac resynchronization therapy: the fallacy of echocardiographic dyssynchrony. *J Am Coll Cardiol.* (2009) 53(21):1944–59. doi: 10.1016/j.jacc.2008.11.062

22. Lim P, Donal E, Lafitte S, Derumeaux G, Habib G, Réant P, et al. Multicentre study using strain delay index for predicting response to cardiac resynchronization therapy (MUSIC study). *Eur J Heart Fail.* (2011) 13(9):984–91. doi: 10.1093/eurjhf/hfr073

23. Bernard A, Donal E, Leclercq C, Schnell F, Fournet M, Reynaud A, et al. Impact of cardiac resynchronization therapy on left ventricular mechanics: understanding the

response through a new quantitative approach based on longitudinal strain integrals. *J Am Soc Echocardiogr.* (2015) 28(6):700–8. doi: 10.1016/j.echo.2015.02.017

24. Risum N, Tayal B, Hansen TF, Bruun NE, Jensen MT, Lauridsen TK, et al. Identification of typical left bundle branch block contraction by strain echocardiography is additive to electrocardiography in prediction of long-term outcome after cardiac resynchronization therapy. *J Am Coll Cardiol.* (2015) 66 (6):631–41. doi: 10.1016/j.jacc.2015.06.020

25. Gorcsan J, Anderson CP, Tayal B, Sugahara M, Walmsley J, Starling RC, et al. Systolic stretch characterizes the electromechanical substrate responsive to cardiac resynchronization therapy. *JACC Cardiovasc Imaging.* (2019) 12(9):1741–52. doi: 10. 1016/j.jcmg.2018.07.013

26. Parsai C, Bijnens B, Sutherland GR, Baltabaeva A, Claus P, Marciniak M, et al. Toward understanding response to cardiac resynchronization therapy: left ventricular dyssynchrony is only one of multiple mechanisms. *Eur Heart J.* (2009) 30(8):940–9. doi: 10.1093/eurheartj/ehn481

27. Stankovic I, Prinz C, Ciarka A, Daraban AM, Kotrc M, Aarones M, et al. Relationship of visually assessed apical rocking and septal flash to response and long-term survival following cardiac resynchronization therapy (PREDICT-CRT). *Eur Heart J Cardiovasc Imaging.* (2016) 17(3):262–9. doi: 10.1093/ehjci/jev288

28. Marsan NA, Westenberg JJM, Ypenburg C, van Bommel RJ, Roes S, Delgado V, et al. Magnetic resonance imaging and response to cardiac resynchronization therapy: relative merits of left ventricular dyssynchrony and scar tissue. *Eur Heart J.* (2009) 30 (19):2360–7. doi: 10.1093/eurheartj/ehp280

29. Parsai C, Baltabaeva A, Anderson L, Chaparro M, Bijnens B, Sutherland GR. Low-dose dobutamine stress echo to quantify the degree of remodelling after cardiac resynchronization therapy. *Eur Heart J.* (2009) 30(8):950–8. doi: 10.1093/ eurheartj/ehp050

30. Ciampi Q, Pratali L, Citro R, Piacenti M, Villari B, Picano E. Identification of responders to cardiac resynchronization therapy by contractile reserve during stress echocardiography. *Eur J Heart Fail.* (2009) 11(5):489–96. doi: 10.1093/eurjhf/hfp039

31. Delgado-Montero A, Tayal B, Goda A, Ryo K, Marek JJ, Sugahara M, et al. Additive prognostic value of echocardiographic global longitudinal and global circumferential strain to electrocardiographic criteria in patients with heart failure undergoing cardiac resynchronization therapy. *Circ Cardiovasc Imaging.* (2016) 9 (6):e004241. doi: 10.1161/CIRCIMAGING.115.004241

32. Khidir MJH, Abou R, Yilmaz D, Ajmone Marsan N, Delgado V, Bax JJ. Prognostic value of global longitudinal strain in heart failure patients treated with cardiac resynchronization therapy. *Heart Rhythm.* (2018) 15(10):1533–9. doi: 10. 1016/j.hrthm.2018.03.034

33. van der Bijl P, Kostyukevich MV, Khidir M, Ajmone Marsan N, Delgado V, Bax JJ. Left ventricular remodelling and change in left ventricular global longitudinal strain after cardiac resynchronization therapy: prognostic implications. *Eur Heart J Cardiovasc Imaging.* (2019) 20(10):1112–9. doi: 10.1093/ehjci/jez072

34. Delgado V, van Bommel RJ, Bertini M, Borleffs CJW, Marsan NA, Ng ACT, et al. Relative merits of left ventricular dyssynchrony, left ventricular lead position, and myocardial scar to predict long-term survival of ischemic heart failure patients undergoing cardiac resynchronization therapy. *Circulation.* (2011) 123(1):70–8. doi: 10.1161/CIRCULATIONAHA.110.945345

35. Khan FZ, Virdee MS, Palmer CR, Pugh PJ, O'Halloran D, Elsik M, et al. Targeted left ventricular lead placement to guide cardiac resynchronization therapy: the TARGET study: a randomized, controlled trial. *J Am Coll Cardiol.* (2012) 59 (17):1509–18. doi: 10.1016/j.jacc.2011.12.030

36. Bose A, Kandala J, Upadhyay GA, Riedl L, Ahmado I, Padmanabhan R, et al. Impact of myocardial viability and left ventricular lead location on clinical outcome in cardiac resynchronization therapy recipients with ischemic cardiomyopathy. *J Cardiovasc Electrophysiol.* (2014) 25(5):507–13. doi: 10.1111/jce.12348

37. Adelstein EC, Tanaka H, Soman P, Miske G, Haberman SC, Saba SF, et al. Impact of scar burden by single-photon emission computed tomography myocardial perfusion imaging on patient outcomes following cardiac resynchronization therapy. *Eur Heart J.* (2011) 32(1):93–103. doi: 10.1093/eurheartj/ehq389

38. Moss AJ, Hall WJ, Cannom DS, Klein H, Brown MW, Daubert JP, et al. Cardiac-resynchronization therapy for the prevention of heart-failure events. *N Engl J Med.* (2009) 361(14):1329–38. doi: 10.1056/NEJMoa0906431

39. Carluccio E, Biagioli P, Alunni G, Murrone A, Pantano P, Biscottini E, et al. Presence of extensive LV remodeling limits the benefits of CRT in patients with intraventricular dyssynchrony. *JACC Cardiovasc Imaging.* (2011) 4(10):1067–76. doi: 10.1016/j.jcmg.2011.07.006

40. Galli E, Smiseth OA, Aalen JM, Larsen CK, Sade E, Hubert A, et al. Prognostic utility of the assessment of diastolic function in patients undergoing cardiac resynchronization therapy. *Int J Cardiol.* (2021) 331:144–51. doi: 10.1016/j.ijcard.2021.01.046

41. Kuperstein R, Goldenberg I, Moss AJ, Solomon S, Bourgoun M, Shah A, et al. Left ventricular volume and the benefit of cardiac resynchronization therapy in the MADIT-CRT trial. *Circ Heart Fail.* (2014) 7(1):154–60. doi: 10.1161/ CIRCHEARTFAILURE.113.000748

42. Galli E, Oger E, Aalen JM, Duchenne J, Larsen CK, Sade E, et al. Left atrial strain is a predictor of left ventricular systolic and diastolic reverse remodelling in CRT

candidates. *Eur Heart J Cardiovasc Imaging*. (2022) 23(10):1373–82. doi: 10.1093/ehjci/jeab163

43. Damy T, Ghio S, Rigby AS, Hittinger L, Jacobs S, Leyva F, et al. Interplay between right ventricular function and cardiac resynchronization therapy: an analysis of the CARE-HF trial (Cardiac resynchronization-heart failure). *J Am Coll Cardiol*. (2013) 61(21):2153–60. doi: 10.1016/j.jacc.2013.02.049

44. Rapacciuolo A, Maffè S, Palmisano P, Ferraro A, Cecchetto A, D'Onofrio A, et al. Prognostic role of right ventricular function in patients with heart failure undergoing cardiac resynchronization therapy: prognostic role of RV function in CRT patients. *Clin Cardiol*. (2016) 39(11):640–5. doi: 10.1002/clc.22574

45. van Everdingen WM, Walmsley J, Cramer MJ, van Hagen I, De Boeck BWL, Meine M, et al. Echocardiographic prediction of cardiac resynchronization therapy response requires analysis of both mechanical dyssynchrony and right ventricular function: a combined analysis of patient data and computer simulations. *J Am Soc Echocardiogr*. (2017) 30(10):1012–20.e2. doi: 10.1016/j.echo.2017.06.004

46. Voigt JU, Schneider TM, Korder S, Szulik M, Gürel E, Daniel WG, et al. Apical transverse motion as surrogate parameter to determine regional left ventricular function inhomogeneities: a new, integrative approach to left ventricular asynchrony assessment. *Eur Heart J*. (2009) 30(8):959–68. doi: 10.1093/eurheartj/ehp062

47. van Oosterhout MF, Prinzen FW, Arts T, Schreuder JJ, Vanagt WY, Cleutjens JP, et al. Asynchronous electrical activation induces asymmetrical hypertrophy of the left ventricular wall. *Circulation*. (1998) 98(6):588–95. doi: 10.1161/01.CIR.98.6.588

48. Stankovic I, Aarones M, Smith HJ, Voros G, Kongsgaard E, Neskovic AN, et al. Dynamic relationship of left-ventricular dyssynchrony and contractile reserve in patients undergoing cardiac resynchronization therapy. *Eur Heart J*. (2014) 35 (1):48–55. doi: 10.1093/eurheartj/eht294

49. Stankovic I, Prinz C, Ciarka A, Daraban AM, Mo Y, Aarones M, et al. Long-term outcome after CRT in the presence of mechanical dyssynchrony seen with chronic RV pacing or intrinsic LBBB. *JACC Cardiovasc Imaging*. (2017) 10(10 Pt A):1091–9. doi: 10.1016/j.jcmg.2016.08.015

50. Mada RO, Lysyansky P, Duchenne J, Beyer R, Mada C, Muresan L, et al. New automatic tools to identify responders to cardiac resynchronization therapy. *J Am Soc Echocardiogr*. (2016) 29(10):966–72. doi: 10.1016/j.echo.2016.06.008

51. AlJaroudi W, Chen J, Jaber WA, Lloyd SG, Cerqueira MD, Marwick T. Nonechocardiographic imaging in evaluation for cardiac resynchronization therapy. *Circ Cardiovasc Imaging*. (2011) 4(3):334–43. doi: 10.1161/CIRCIMAGING.111.963504

52. Kowallick JT, Morton G, Lamata P, Jogiya R, Kutty S, Hasenfuß G, et al. Quantitative assessment of left ventricular mechanical dyssynchrony using cine cardiovascular magnetic resonance imaging: inter-study reproducibility. *JRSM Cardiovasc Dis*. (2017) 6:204800401771014. doi: 10.1177/2048004017710142

53. Galli E, Baritussio A, Sitges M, Donnellan E, Jaber WA, Gimelli A. Multi-modality imaging to guide the implantation of cardiac electronic devices in heart failure: is the sum greater than the individual components? *Eur Heart J Cardiovasc Imaging*. (2023) 24(2):163–76. doi: 10.1093/ehjci/jeac237

54. Park JH, Negishi K, Grimm RA, Popovic Z, Stanton T, Wilkoff BL, et al. Echocardiographic predictors of reverse remodeling after cardiac resynchronization therapy and subsequent events. *Circ Cardiovasc Imaging*. (2013) 6(6):864–72. doi: 10.1161/CIRCIMAGING.112.000026

55. Appadurai V, D'Elia N, Mew T, Tomlinson S, Chan J, Hamilton-Craig C, et al. Global longitudinal strain as a prognostic marker in cardiac resynchronisation therapy: a systematic review. *Int J Cardiol Heart Vasc*. (2021) 35:100849. doi: 10.1016/j.ijcha.2021.100849

56. Bazoukis G, Thomopoulos C, Tse G, Tsioufis K, Nihoyannopoulos P. Global longitudinal strain predicts responders after cardiac resynchronization therapy-a systematic review and meta-analysis. *Heart Fail Rev*. (2022) 27(3):827–36. doi: 10.1007/s10741-021-10094-w

57. Goldenberg I, Moss AJ, Hall WJ, Foster E, Goldberger JJ, Santucci P, et al. Predictors of response to cardiac resynchronization therapy in the multicenter automatic defibrillator implantation trial with cardiac resynchronization therapy (MADIT-CRT). *Circulation*. (2011) 124(14):1527–36. doi: 10.1161/CIRCULATIONAHA.110.014324

58. Martens P, Nijst P, Verbrugge FH, Dupont M, Tang WHW, Mullens W. Profound differences in prognostic impact of left ventricular reverse remodeling after cardiac resynchronization therapy relate to heart failure etiology. *Heart Rhythm*. (2018) 15(1):130–6. doi: 10.1016/j.hrthm.2017.08.021

59. Bakos Z, Ostenfeld E, Markstad H, Werther-Evaldsson A, Roijer A, Arheden H, et al. A comparison between radial strain evaluation by speckle-tracking echocardiography and cardiac magnetic resonance imaging, for assessment of suitable segments for left ventricular lead placement in cardiac resynchronization therapy. *Europace*. (2014) 16(12):1779–86. doi: 10.1093/europace/euu167

60. Koepfli P, Wyss CA, Gaemperli O, Siegrist PT, Klainguti M, Schepis T, et al. Left bundle branch block causes relative but not absolute septal underperfusion during exercise. *Eur Heart J*. (2009) 30(24):2993–9. doi: 10.1093/eurheartj/ehp372

61. Fyenbo DB, Sommer A, Kühl JT, Kofoed KF, Nørgaard BL, Kronborg MB, et al. Transmural myocardial scar assessed by cardiac computed tomography: predictor of

echocardiographic versus clinical response to cardiac resynchronization therapy? *J Comput Assist Tomogr*. (2019) 43(2):312–6. doi: 10.1097/RCT.0000000000000824

62. Bakos Z, Markstad H, Ostenfeld E, Carlsson M, Roijer A, Borgquist R. Combined preoperative information using a bullseye plot from speckle tracking echocardiography, cardiac CT scan, and MRI scan: targeted left ventricular lead implantation in patients receiving cardiac resynchronization therapy. *Eur Heart J Cardiovasc Imaging*. (2014) 15(5):523–31. doi: 10.1093/ehjci/jet233

63. Borgquist R, Carlsson M, Markstad H, Werther-Evaldsson A, Ostenfeld E, Roijer A, et al. Cardiac resynchronization therapy guided by echocardiography, MRI, and CT imaging: a randomized controlled study. *JACC Clin Electrophysiol*. (2020) 6 (10):1300–9. doi: 10.1016/j.jacep.2020.05.011

64. Fyenbo DB, Sommer A, Nørgaard BL, Kronborg MB, Kristensen J, Gerdes C, et al. Long-term outcomes in a randomized controlled trial of multimodality imaging-guided left ventricular lead placement in cardiac resynchronization therapy. *Europace*. (2022) 24(5):828–34. doi: 10.1093/europace/euab314

65. Nagueh SF. Noninvasive estimation of LV filling pressures in heart failure and reduced ejection fraction: revisited and verified. *JACC Cardiovasc Imaging*. (2011) 4 (9):935–7. doi: 10.1016/j.jcmg.2011.06.018

66. Andersen OS, Smiseth OA, Dokainish H, Abudiab MM, Schutt RC, Kumar A, et al. Estimating left ventricular filling pressure by echocardiography. *J Am Coll Cardiol*. (2017) 69(15):1937–48. doi: 10.1016/j.jacc.2017.01.058

67. Egnaczyk GF, Chung ES. The relationship between cardiac resynchronization therapy and diastolic function. *Curr Heart Fail Rep*. (2014) 11(1):64–9. doi: 10.1007/s11897-013-0181-5

68. Brenyo A, Link MS, Barsheshet A, Moss AJ, Zareba W, Wang PJ, et al. Cardiac resynchronization therapy reduces left atrial volume and the risk of atrial tachyarrhythmias in MADIT-CRT (Multicenter automatic defibrillator implantation trial with cardiac resynchronization therapy). *J Am Coll Cardiol*. (2011) 58 (16):1682–9. doi: 10.1016/j.jacc.2011.07.020

69. Valzania C, Gadler F, Boriani G, Rapezzi C, Eriksson MJ. Effect of cardiac resynchronization therapy on left atrial size and function as expressed by speckle tracking 2-dimensional strain. *Am J Cardiol*. (2016) 118(2):237–43. doi: 10.1016/j.amjcard.2016.04.042

70. Sharma A, Bax JJ, Vallakati A, Goel S, Lavie CJ, Kassotis J, et al. Meta-analysis of the relation of baseline right ventricular function to response to cardiac resynchronization therapy. *Am J Cardiol*. (2016) 117(8):1315–21. doi: 10.1016/j.amjcard.2016.01.029

71. Storsten P, Aalen JM, Boe E, Remme EW, Gjesdal O, Larsen CK, et al. Mechanical Effects on Right Ventricular Function From Left Bundle Branch Block and Cardiac Resynchronization Therapy. JACC Cardiovasc Imaging [Internet].(2020) [cité 4 mai 2020]; Disponible sur:. Available from: https://linkinghub.elsevier.com/retrieve/pii/S1936878X19310496

72. Naeije R, Badagliacca R. The overloaded right heart and ventricular interdependence. *Cardiovasc Res*. (2017) 113(12):1474–85. doi: 10.1093/cvr/cvx160

73. Krittanawong C, Zhang H, Wang Z, Aydar M, Kitai T. Artificial intelligence in precision cardiovascular medicine. *J Am Coll Cardiol*. (2017) 69(21):2657–64. doi: 10.1016/j.jacc.2017.03.571

74. Eckhardt LL, Kalscheur MM. Machine learning in CRT outcomes: implementing the right tool for the right outcome. *JACC Clin Electrophysiol*. (2021) 7(12):1516–8. doi: 10.1016/j.jacep.2021.08.003

75. Donal E, Hubert A, Le Rolle V, Leclercq C, Martins R, Mabo P, et al. New multiparametric analysis of cardiac dyssynchrony: machine learning and prediction of response to CRT. *JACC Cardiovasc Imaging*. (2019) 12(9):1887–8. doi: 10.1016/j.jcmg.2019.03.009

76. Gallard A, Hubert A, Smiseth O, Voigt JU, Le Rolle V, Leclercq C, et al. Prediction of response to cardiac resynchronization therapy using a multi-feature learning method. *Int J Cardiovasc Imaging*. (2021) 37(3):989–98. doi: 10.1007/s10554-020-02083-1

77. Gallard A, Galli E, Hubert A, Bidaut A, Le Rolle V, Smiseth O, et al. Echocardiographic view and feature selection for the estimation of the response to CRT. *PLoS One*. (2021) 16(6):e0252857. doi: 10.1371/journal.pone.0252857

78. Cikes M, Sanchez-Martinez S, Claggett B, Duchateau N, Piella G, Butakoff C, et al. Machine learning-based phenogrouping in heart failure to identify responders to cardiac resynchronization therapy. *Eur J Heart Fail*. (2019) 21(1):74–85. doi: 10.1002/ejhf.1333

79. Galli E, Le Rolle V, Smiseth OA, Duchenne J, Aalen JM, Larsen CK, et al. Importance of systematic right ventricular assessment in cardiac resynchronization therapy candidates: a machine learning approach. *J Am Soc Echocardiogr*. (2021) 34 (5):494–502. doi: 10.1016/j.echo.2020.12.025

80. Bivona DJ, Tallavajhala S, Abdi M, Oomen PJA, Gao X, Malhotra R, et al. Machine learning for multidimensional response and survival after cardiac resynchronization therapy using features from cardiac magnetic resonance. *Heart Rhythm*. (2022) 3(5):542–52. doi: 10.1016/j.hroo.2022.06.005

81. Owashi K, Taconné M, Courtial N, Simon A, Garreau M, Hernandez A, et al. Desynchronization strain patterns and contractility in left bundle branch block through computer model simulation. *J Cardiovasc Dev Dis*. (2022) 9(2):53. doi: 10.3390/jcdd9020053

82. Lumens J, Leenders GE, Cramer MJ, De Boeck BWL, Doevendans PA, Prinzen FW, et al. Mechanistic evaluation of echocardiographic dyssynchrony indices: patient data combined with multiscale computer simulations. *Circ Cardiovasc Imaging.* (2012) 5(4):491–9. doi: 10.1161/CIRCIMAGING.112.973446

83. Le Rolle V, Hernández AI, Richard PY, Donal E, Carrault G. A tissue-level model of the left ventricle for the analysis of regional myocardial function. *Annu Int Conf IEEE Eng Med Biol Soc.* (2007) 2007:1172–5. doi: 10.1109/IEMBS.2007. 4352505

84. Sermesant M, Chabiniok R, Chinchapatnam P, Mansi T, Billet F, Moireau P, et al. Patient-specific electromechanical models of the heart for the prediction of pacing acute effects in CRT: a preliminary clinical validation. *Med Image Anal.* (2012) 16(1):201–15. doi: 10.1016/j.media.2011.07.003

85. Khamzin S, Dokuchaev A, Bazhutina A, Chumarnaya T, Zubarev S, Lyubimtseva T, et al. Machine learning prediction of cardiac resynchronisation therapy response from combination of clinical and model-driven data. *Front Physiol.* (2021) 12:753282. doi: 10.3389/fphys.2021.753282

86. Lee AWC, Costa CM, Strocchi M, Rinaldi CA, Niederer SA. Computational modeling for cardiac resynchronization therapy. *J Cardiovasc Transl Res.* (2018) 11 (2):92–108. doi: 10.1007/s12265-017-9779-4

87. Armeni P, Polat I, De Rossi LM, Diaferia L, Meregalli S, Gatti A. Digital twins in healthcare: is it the beginning of a new era of evidence-based medicine? A critical review. *J Pers Med.* (2022) 12(8):1255. doi: 10.3390/jpm12081255

88. Rajkomar A, Dean J, Kohane I. Machine learning in medicine. *N Engl J Med.* (2019) 380(14):1347–58. doi: 10.1056/NEJMra1814259

89. de Souza Filho EM, de Amorim Fernandes F, de Assis Pereira NC, Mesquita CT, Gismondi RA. Ethics, artificial intelligence and cardiology. *Arq Bras Cardiol.* (2020) 115(3):579–83. doi: 10.36660/abc.20200143

90. Mullens W, Auricchio A, Martens P, Witte K, Cowie MR, Delgado V, et al. Optimized implementation of cardiac resynchronization therapy: a call for action for referral and optimization of care: a joint position statement from the heart failure association (HFA), European heart rhythm association (EHRA), and European association of cardiovascular imaging (EACVI) of the European society of cardiology. *Eur J Heart Fail.* (2020) 22(12):2349–69. doi: 10.1002/ejhf.2046